

## Development of a Magnetic Field Probe for Near-Field Measurement

Goh Kai Loon<sup>a</sup> & Mohd Hafiz Baharuddin\*

<sup>a</sup>Department of Electrical, Electronic and System Engineering,

Faculty of Engineering & Built Environment, Universiti Kebangsaan Malaysia, Malaysia

\*Corresponding authors: hafizb@ukm.edu.my

Received 08 October 2020, Received in revised form 28 December 2020  
Accepted 28 January 2021, Available online 30 November 2021

### ABSTRACT

Current electronic circuits are characterised by their compact design of miniaturisation; however, such a feature has also contributed to the rise of electromagnetic compatibility issues. This study introduces a technique to develop a magnetic field probe for near-field measurement. The probe aims at performing the debugging of electromagnetic interference on an integrated circuit. Certain processes, such as designing a microstrip line in simulation and a prototype for the validation as well as developing a functional magnetic field probe for near-field scanning and calibration measurement to determine the probe factor, have been performed under a frequency domain. The microstrip line model is built both as a simulation and a real prototype, and the handcrafted loop probe is developed with the same diameter as a commercial probe. Calibration measurement is set-up with a vector network analyser (VNA) to capture the magnetic field on radiated plane. The performance of the handcrafted probe in terms of measuring the configuration of the H-field source on the scattering region is conducted. Two types of measurements which are S11 and S21 will be conducted using a VNA. The comparison of the S11 and S21 results against simulation results are plotted using MATLAB. S11 represents the return loss of the microstrip line while S21 represents the power received by the magnetic field probe relative to power input to the microstrip line. The results of the S11 parameter indicate that the customised microstrip line board has a similar waveform pattern that matches the one on the simulation model. The S21 results for the handcrafted probe revealed that it can only function well up to the frequency of 2.644 GHz, the abnormal result obtained after the frequency mentioned. Some factors may have affected the results, such as material loss, fabrication tolerance and interferences from other devices. Therefore, calibration measurement is conducted under a less reflected radiation environment, and the designated substrate should be a perfect material correlated with the measurement.

*Keywords:* Electromagnetic compatibility issues; microstrip line; handcrafted loop probe

### INTRODUCTION

Overall, technology in this century is more advanced and sophisticated in every field compared with the predecessors. Electronic circuits are required in every existing technologies to help them function in accordance with their design. However, there has been an increase in interference problems in integrated circuits (ICs) due to the trend of compact design and miniaturisation. Therefore, these ICs are required to function in close proximity to one another, and the interference problems might affect their adjacent components. This interference issue is known as the

electromagnetic radiation (EMR), which is defines as the waves of the electromagnetic field propagating across space and bearing EMR energy (Purcell & Morin 2013). Electromagnetic waves of different frequencies are called by different names, as they have various sources and impacts on matter (Siegel & Siegel 2009).

Magnetic field probes are commonly used in electromagnetic compatibility (EMC) diagnostic work. Since the 1920s, the methods of radio communication and direction findings have been derived from antennas with different configurations and features, although they are still electrically small shielded loop antennas (Roy Ediss, Philips Semiconductors 1939). For near-field measurements,

a miniature magnetic loop probe with a single turn is often used. The standard probe consists of a wire, coaxial cable, PCB traces and any other suitable material. Figure 1 shows the equivalent circuit of the discrete magnetic field probe and its output. However, when the magnetic flux enters the loop section, this generates the current produced by the magnetic field called the induced current ( $I_m$ ). The magnetic field is induced at the magnetic probe's output signal. The magnetic field is induced at the magnetic probe's output signal (Electrotechnical & Commission 2014).

The magnetic field probe is the most important part of a near field measurement system that is used to characterise radiation from electronic devices. In (Li et al. 2015), the magnetic field probe was used to extract near field scanning data in order to characterise the radiation of source IC. The multipole expansion of a radiated emission study has shown that an arbitrary electrically small source can be represented by roughly a few types of dipoles, which are magnetic dipoles through x, y and z. These dipoles are presented under the Cartesian coordinate system. There are identical fields generated by the dipole sets with the real source. The source of disturbance is defined as the working IC (Li et al. 2015). Figure 2 shows the equivalent dipole moment model arrangement with scanning lane, and Figure 3 shows scanning with a single probe placed vertically above the DUT. Previously, near-field to far field transformation method and equivalent source methods have been proposed to improve the use of the near-field measurement technique (Sivaraman 2017).

In this project, only one handcrafted magnetic field probe is developed for the near-field measurement. The examples of commercial and handcrafted magnetic field probes are shown in Figures 4 and 5. The current study aims to develop a magnetic field probe for near-field measurement. Although commercial magnetic field probes are already available in the market, they are very expensive and limited in terms of size or dimension. Developing a functional magnetic field probe would be useful as it can be designed based on the specific characteristic of the device being tested. A microstrip line is also constructed and built in 3D EM simulation and as a prototype for further validation. The calibration measurement and validation measurement processes are discussed along with the determination of the probe calibration factor. All simulations and measurements are performed in the frequency domain, and MATLAB is also used in the algorithm development. The comparison results with simulation and measurements are discussed and evaluated in this study.

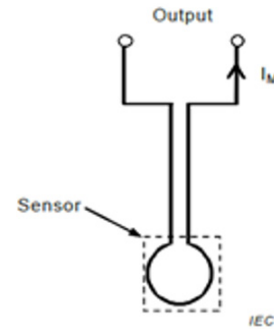


FIGURE 1. Magnetic field probe schematic  
Source: Electrotechnical & Commission (2014)

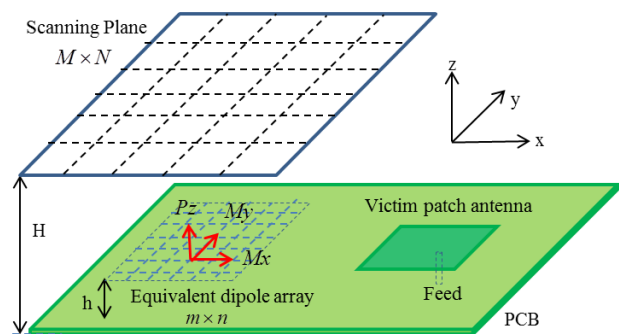


FIGURE 2. The equivalent dipole moment model arrangement with scanning plane  
Source: Li et al. (2015)

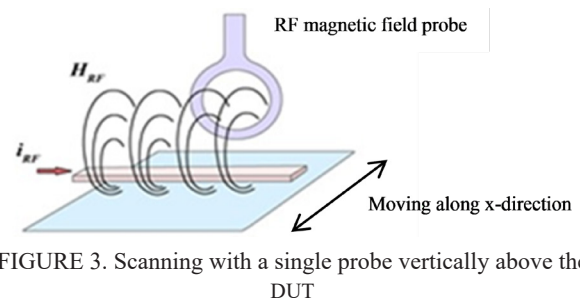


FIGURE 3. Scanning with a single probe vertically above the DUT  
Source: (Hacker & Gmbh 2020)



FIGURE 4. Commercial magnetic field probe  
Source: Ag (2020)



FIGURE 5. Handcrafted magnetic field probe  
Source: Neilhao (2013)

## METHODOLOGY

This section explains the measurement process. The measurements of the  $S_{11}$  and  $S_{21}$  parameters were generated in two different categories: the simulation part and the hands-on experiment part. In the former, the results were simulated through the 3DEM simulation software, whereas in the latter, the data were generated with the use of the vector network analyser (VNA) in the laboratory.

The operating frequency range of 30 MHz to 3 GHz was initially defined in the simulation and measurements. The microstrip line was constructed using 3DEM simulation software, and a prototype of the same design was built for measurements. The handcrafted and commercial magnetic field probe were used with the same diameter. Next, the calibration and validation measurements were conducted in laboratory. The probe is designed to capture the voltages from the measurement using VNA hence the need for the calibration measurement to convert the captured voltages to magnetic fields. From the calibration process, frequency dependent and complex-valued probe calibration factor (PF) are obtained (Zhang et al. 2013). Validation measurement on the other hand is used to test the accuracy of the PF obtained from the calibration measurement at the frequency of 1, 2 and 3 GHz. The measured results were then compared to the simulated results with the algorithm developed in MATLAB.

### DESIGNING THE MICROSTRIP MODEL FOR SIMULATION AND MEASUREMENTS

A microstrip consists of 3 different layers: a conductive strip and conductive ground layer separated by a dielectric layer as the substrate. The physical characteristics of the transmission line trace and the dielectric characteristics must be measured together to obtain the correct impedance values for the circuit (Team 2017). Figure 6 shows a sample microstrip line.

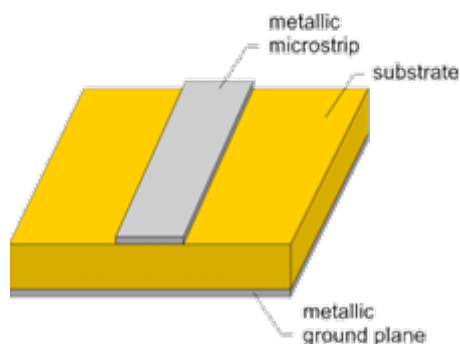


FIGURE 6. A sample microstrip line  
Source: (Brochure 2020)

The impedance requirement for the microstrip line is approximately  $50 \Omega$ . This can be computed using Equations (1) to (3).

$$\text{Since } \left(\frac{W}{H}\right) > 1, \quad (1)$$

$$\epsilon_{eff} = \frac{\epsilon_R + 1}{2} + \left( \frac{\epsilon_R - 1}{2\sqrt{1 + 12\left(\frac{H}{W}\right)}} \right), \quad (2)$$

$$Z_o = \frac{120\pi}{\sqrt{\epsilon_{eff}} \left( \frac{W}{H} + 1.393 + \frac{2}{3} \ln\left(\frac{W}{H} + 1.444\right) \right)}, \quad (3)$$

where  $W$  is width,  $H$  is height,  $\epsilon_k$  is the dielectric constant,  $\epsilon_{eff}$  is the effective dielectric constant, and  $Z_o$  is the impedance.

The calculated impedance value is shown in Table 1.

TABLE 1. Impedance value based on equations

	Result
Width/Height	1.906
Effective dielectric constant, $\epsilon_{eff}$	3.466
Impedance, $Z_o$	49.32 $\Omega$

Table 2 depicts some other parameters that are also required in constructing the model in simulation. Figure 7 shows the microstrip line used for the measurements.

TABLE 2. List of parameters used for designing the microstrip line model

Microstrip line	Parameters
Dielectric constant (FR-4-loss free)	4.60 (Epsilon_r)
Length	160 mm
Substrate height	1.60 mm
Trace width	3.05 mm
Trace thickness	0.10 mm
Ground thickness	0.10 mm
Substrate width	100 mm

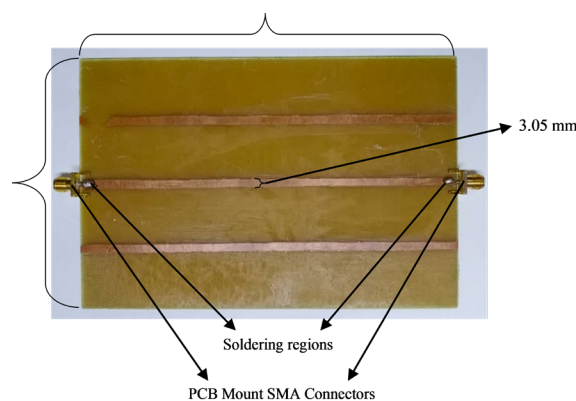


FIGURE 7. Microstrip line used for the measurements

## DEVELOPING A HANDCRAFTED MAGNETIC FIELD PROBE FOR MEASUREMENTS

A magnetic field probe is a measuring instrument that is used to study and test electromagnetic fields. Such a probe tests and measures the strength of the electromagnetic field and gives relational X, Y and Z as well as total field values.

Figures 8 and 9 describe the coaxial cable cutaway and the creating loop from within the coax cable.

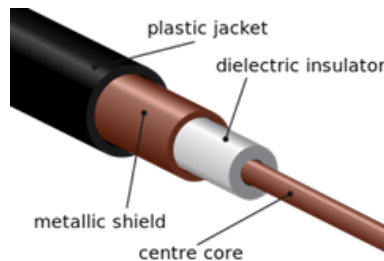


FIGURE 8. Coaxial cable cutaway  
Source: Shrestha (2009)

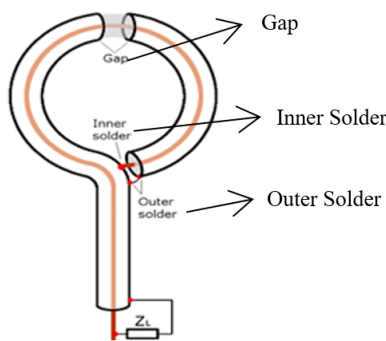


FIGURE 9. Creating a loop from the coax cable  
Source: Oliveira (2018)

In this project, the process of designing and developing a handcrafted magnetic field probe from 1 meter of  $50 \Omega$  RG405 coax cable is described. First, the cable was cut down, and the shield conductive layer (as outer braid) and the dielectric in the middle were removed at one end of the cable. This was followed by retaining and shorting out the inner conductor of the coaxial cable and exposing a small amount over the other end. Meanwhile, in order to form a circular radius, it is bent back at a 90-degree angle to create a closed loop with a diameter of 10 mm. The inner conductor and outer shield (as shielding conductive layer) were literally soldered together; hence, the connection between them was shorted out. Once the soldering work was done, it was important to keep an extremely small slot as small as possible (around a millimetre) in the outer sheath of the centre of the loop. A commercial field probe was also used in the measurement as required to make the comparison result with the handcrafted one.

For this project, however, only small probes with a diameter of 10 mm were tested and measured. This served

as a good sample to compare with a commercial probe having the same diameter.

## TESTING AND MEASUREMENTS

Once the designing and developing works were completed, the calibration and validation measurements were performed. All the required equipment for the measurements were set up for the experiment. The measurements were done using two similar 10-mm loop probes: a commercial magnetic field probe and a handcrafted loop probe made from a coaxial cable.

### a. Set-up of the Near-Field Measurement

The proposed measurement method used the automated frequency domain measurement. It was performed in the near-field lab at the Universiti Kebangsaan Malaysia.

In this experiment, VNA was used to measure the response of the results in the vector form with real and imaginary parameters in the form of S-parameters ( $S_{11}$  and  $S_{21}$ ). Measurements were set with a frequency range of 30 MHz to 3 GHz. The near-field measurement system consisted of scanning probes (commercial and handcrafted probes), a VNA and a 3D positioning printing system. The setup of the frequency domain scanning of H-field scanning is shown in Figure 10.

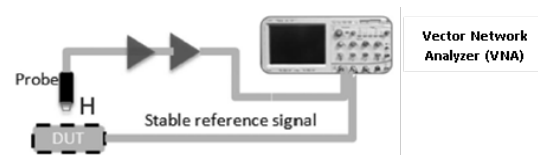


FIGURE 10. Set-up of the frequency domain scanning of H-field scanning  
Source: (Zhang et al. 2013)

A microstrip board with  $50 \Omega$  load was chosen as the test structure. A precise analytical solution and full-wave simulation were acquired from the field distribution above the microstrip board. Meanwhile, with the FR-4 dielectric as the substrate, this microstrip line was fabricated with the following characteristics: substrate relative permittivity  $\epsilon_r = 4.6$ , strip line width  $W = 3.05$  mm, substrate height  $H = 1.60$  mm and length  $L = 160$  mm. The microstrip line used for the measurement is shown in Figure 11.

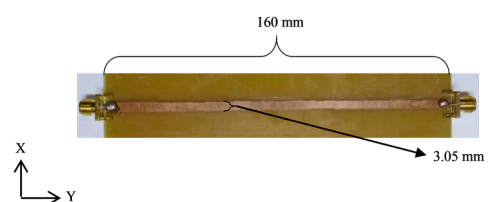


FIGURE 11. The microstrip line used for the near-field measurement

b. Calibration Measurements

- Position Fixed at Height  $z = 15$  mm

For the measurement, the scanning probe was fixed at a height  $z = 15$  mm above the centre of the microstrip line with  $x$  and  $y$  at the origin. The line was mounted along the  $y$ -axis with the length  $L = 160$  mm, as mentioned earlier. One of its terminals was connected with 50 Ohm load, and the other one was connected to the VNA output port (Port 1). Meanwhile, the VNA input port (Port 2) was linked to the magnetic field loop probe. The data obtained by the VNA were correlated to the  $S_{21}$  parameter of the two ports. These were further analysed and manipulated to obtain the response of the probe as voltage that was used to measure and evaluate the PF. Figure 12 below shows the loop probes placed at height  $z = 15.0$  mm above the strip line from the centre of the loop (radius  $r = 5.0$  mm).

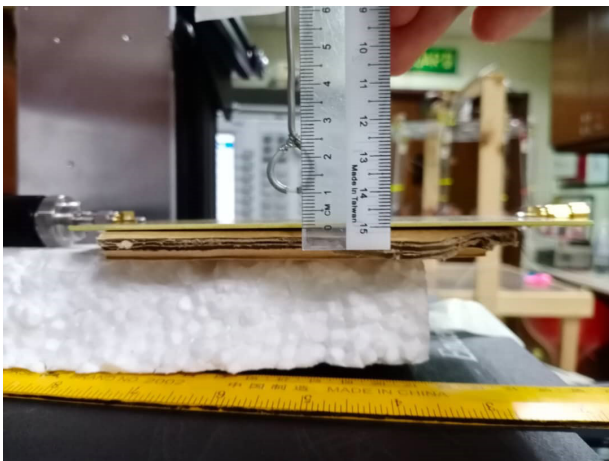


FIGURE 12. The loop probe was placed at height  $z = 15.0$  mm above the strip line from the centre of the loop (radius,  $r = 5.0$  mm)

The equation below is the probe calibration factor equation. This was used to determine the H-field from the captured voltage in measurement data

$$PF = \frac{V}{H} \tag{4}$$

where  $V$  is the captured voltage and  $H$  is field strength. However, the  $S_{21}$  parameter is a measure of power transfer from Port 1 to Port 2. Figure 13 shows the S-parameters of the 2-port network.

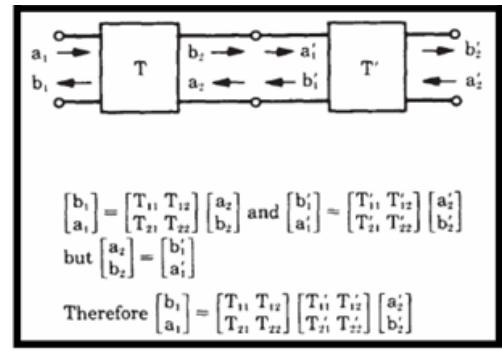
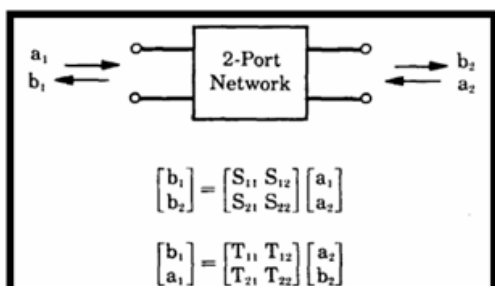


FIGURE 13. S-Parameter of 2-Port Network  
Source: (Huang 2019)

- Positioning across the X-Direction at Height  $z = 15$  mm

In this measurement, the loop probe was placed at a fixed height  $z = 15.0$  mm vertically above the microstrip board from the centre of the loop. This was then moved along the  $x$ -direction with the help of a 3D positioning system. However, the  $y$ -direction was maintained at the origin and a fixed height, as mentioned earlier. This calibration was done with two similar 10-mm probes (commercial and handcrafted). The data obtained were the measured voltage signals, which were further used for the validation measurement. The probe was positioned vertically close to the microstrip line and then moved in order to capture a large set of distribution field data on a surface plane above the microstrip board.

c. Validation Measurement

The validation measurement was based on the probe calibration factor obtained from the calibration results. The purpose of conducting the validation was to test the ability of the loop probe to work properly as the ideal magnetic field probe. This validation was meant to convert the measured voltage signal to the required H-field as in the simulation, after which the differences can be compared against the simulation data. The comparison of the differences was conducted through MATLAB simulation with few mathematical applications. The results were plotted in a graph.

## RESULTS AND DISCUSSION

### CALIBRATION RESULTS AND DATA

For the calibration measurement, the data in S-parameters from simulation and measurements were processed by data aggregation using MATLAB coding in the validation process. All data were obtained in the frequency domain. In addition, in the Cartesian coordinates, the  $S_{11}$  parameter was used for only the microstrip line, and the  $S_{21}$  parameter was used for obtaining the tangential magnetic field, i.e.  $H_x$  from the near-field plane source.

a. Measurement on the Microstrip Line ( $S_{11}$  Parameter Matrix)

Figure 14 depicts the combined plotted graphs of the microstrip lines from the simulations and measurements. The waveguides for  $S_{11}$  can be fed on the transmission line in order to fulfil the S-parameter reference planes that were used in the simulation with those used in the scanning measurement described on the VNA. However, the purpose of the full-wave simulation was to obtain the numeric field data to be compared with the measured  $S_{11}$ .

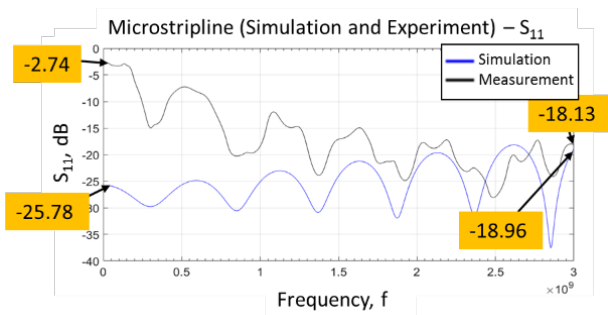


FIGURE 14. Simulated and measured  $S_{11}$  for both waveguides

From the comparison graph, the measured field in  $S_{11}$  has a similar waveform pattern that matches the simulated wave pattern. At the starting point at frequency 30 MHz, both simulated and measured start at magnitudes of  $-25.78$  and  $-2.74$  dB respectively. However, at the end point of 3 GHz, they both ended at the corresponding magnitudes of  $-18.96$  and  $-18.13$  dB. Both wave graphs are approaching the similar wave pattern.

Such a result can be attributed to the fact that the plotted graph was not as smooth as that simulated under the same S-parameter reference microstrip line, as it was developed and customised from a double-sided plain copper board. Some other factors, such as material loss, fabrication tolerance, SMA soldering and some frequency shift or noises distributed from nearby component during the measurement, may have affected the measurement results.

However, the difference between these findings does not have as great of an impact, because the frequency lies within the same frequency band required to enable the microstrip line to function. Therefore, the measured  $S_{11}$  for the measurement is still considered as the accepted result, as it contains the similar wave pattern to the simulated  $S_{11}$  in dB versus the frequency curve result.

b. Measurement for the Fixed Position ( $S_{21}$  Parameter Matrix)

Figure 15 shows the comparison of the  $S_{21}$  parameters of the simulated, commercial and handcrafted probes within the frequency range of 30 MHz to 3 GHz.

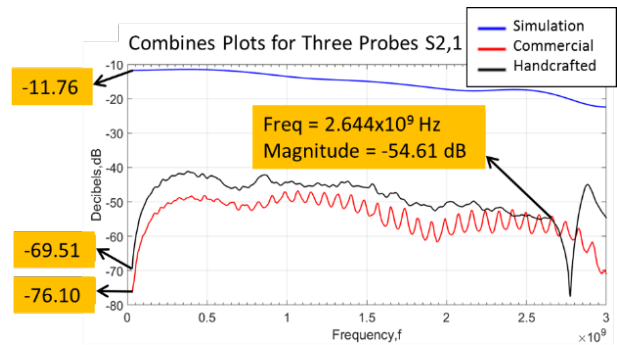


FIGURE 15.  $S_{21}$  parameters of the simulated, commercial and handcrafted probes

At 30 MHz, the simulated H is at  $-11.76$  dBA/m, meanwhile, the measured H for the commercial and handcrafted probes are  $-76.1$  and  $-69.51$  dBV, respectively. Based on the graph above, the measured handcrafted probe gives the similar waveform pattern as the commercial probe just before it reaches the frequency of 2.644 GHz at a magnitude of  $-54.61$  dBV. There is a noticeable decrease after 2.644 GHz, which means that the handcrafted loop probe can only be working properly just before that frequency. The losses due to the feed connector and the coaxial cable might be the reason for the handcrafted probe obtaining such responses on the microstrip line. Furthermore, having the worst surroundings and a great deal of reflection phenomena greatly influenced the outcome. As the scanning measurement was conducted in the laboratory, the presence of numerous metallic objects may have significantly affected the outcome due to the many reflected signals that disturbed the scanning measurement. Nevertheless, such results can still be used in comparing the commercial and handcrafted magnetic field probes.

Figure 16 illustrates the PF for the handcrafted loop probe.

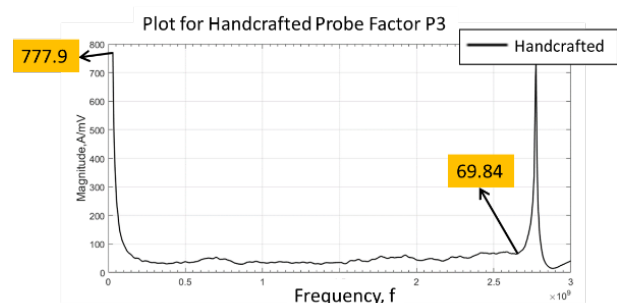


FIGURE 16. Probe calibration factor for the handcrafted loop probe

The PF was calculated using the ratio of simulated complex-valued H-signal to the measured complex-valued voltage signal, thus yielding the resultant PF unit in magnitude (A/mV). The calculation was also conducted through MATLAB coding and then converted in magnitude versus frequency. The PF at 30 MHz is 777.9 dBA/mV. When it reaches a frequency of 2.644 GHz with magnitude of

69.84 dB, there occurs a significant change in the graph. This shows that the handcrafted probe is not working well in the frequency range of 2.644 to 3 GHz.

c. Measurement for the Position across the Hx-Direction ( $S_{21}$  Parameter Matrix)

The commercial and handcrafted loop probes were positioned and moved along the Hx-direction with the interval of 21 points taken on the plane tangentially above the microstrip board ( $H_z = 15$  mm,  $H_y = 0$ ). The data obtained were further processed using MATLAB routines to calculate and compute the measured H-field in the position interval from 1 to 101 points. This is because the simulated H field along the Hx plane on the constructed model has the interval points of 1 to 101. The positions on the measured results were required to change the ongoing interpolation process using MATLAB, thus matching with the interval position in the simulated one.

Figure 17 illustrates the measured voltages for two probes along the Hx direction above the microstrip board at frequencies of 1 and 2 GHz, respectively.

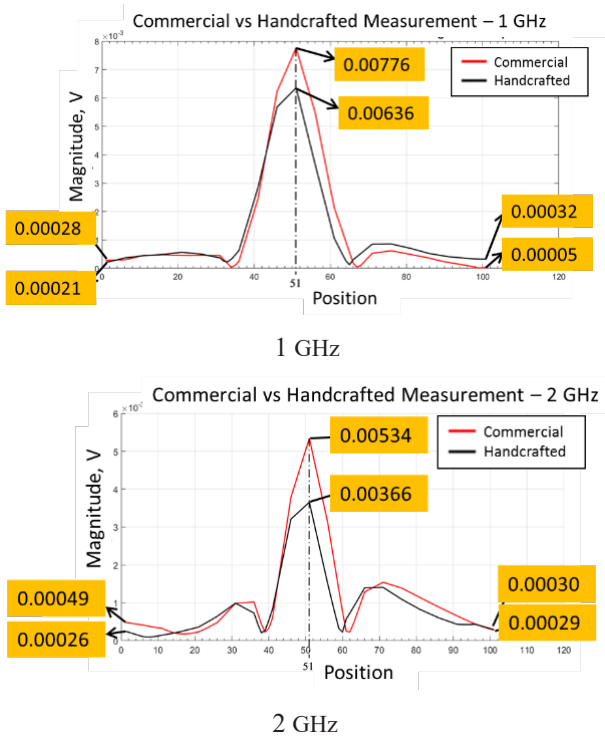


FIGURE 17. Commercial and handcrafted probes across the Hx-direction at frequencies of 1 and 2 GHz

As can be seen, at frequencies of 1 and 2 GHz, the commercial probe has good sensitivity and accuracy in the scanned measurement as compared to the handcrafted loop probe. During the measurement at 1 GHz, the measured voltages in magnitude (decibels, dB) for the commercial and handcrafted probes are  $7.76 \times 10^{-3}$  and  $6.357 \times 10^{-3}$  dBV, respectively. At 2 GHz, the commercial probe has better

sensitivity at  $5.344 \times 10^{-3}$  dBV compared to the handcrafted probe at  $3.656 \times 10^{-3}$  dBV. In both 1 and 2 GHz frequencies, they have the same waveform patterns, indicating that the handcrafted probe can still be functioning properly in the scanned measurement.

Figure 18 depicts the measured voltages for the two probes along the Hx direction above the microstrip board at a frequency of 3 GHz. However, the magnitude of the handcrafted probe is  $4.095 \times 10^{-3}$  dB and that of the commercial probe is  $3.181 \times 10^{-3}$  dB. In accordance with the previous result in the measurement for fixed position, the handcrafted probe is unable to properly measure between the frequency range of 2.644 GHz and 3 GHz. Therefore, it also yields the same result in the measurement along the Hx-direction for the frequency of 3 GHz. The waveform pattern for the handcrafted probe shown in the result is abnormal compared to that of the commercial probe.

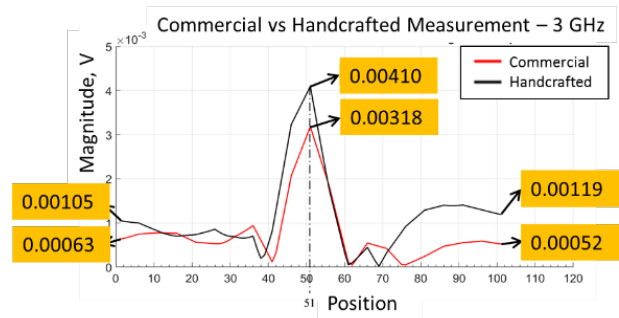


FIGURE 18. Commercial and handcrafted probes across the Hx-direction for the frequency of 3 GHz

Table 3 shows the respective magnitudes of the commercial and handcrafted probes for the measurements along the Hx-direction at 1, 2 and 3 GHz frequencies.

TABLE 3. The maximum magnitude for both probes at point 51 and frequencies of 1, 2 and 3 GHz

Frequency, GHz	At Point 51	
	Commercial, (dB) <i>mV</i>	Handcrafted, (dB) <i>mV</i>
1	7.760	6.357
2	5.344	3.656
3	4.095	3.181

VALIDATION OF THE SIMULATION AND HANDCRAFTED FIELD PROBE

The validation of this measurement was done based on calibration PF. In this topic, only the handcrafted loop probe results were used to compare its ability to obtain the data with the simulated results at three different frequencies of (1, 2 and 3 GHz). Figure 19 shows the simulated and measured results of  $S_{21}$  at frequencies of 1 and 2 GHz after

applying the PF to the measured voltage. It can be observed that the measured field magnitude of the measurement is almost similar to the simulated field strength. For 1 GHz, the simulated one has a maximum magnitude of 0.2546 dB, and the actual measured value is at 0.2217 dB. For 2 GHz, the simulated one is 0.1726 dB, and the measured is 0.1623 dB. The waveform of the simulated strength is smoother than the measured one. This may be due to the simulated radiated field containing more array data structure as compared to the measured field based on the VNA. During the optimized probing position in calibration measurement, 21 points were taken across the microstrip trace. Therefore, the handcrafted loop probe provides good results in detecting the radiated field on microstrip trace at frequencies of 1 and 2 GHz.

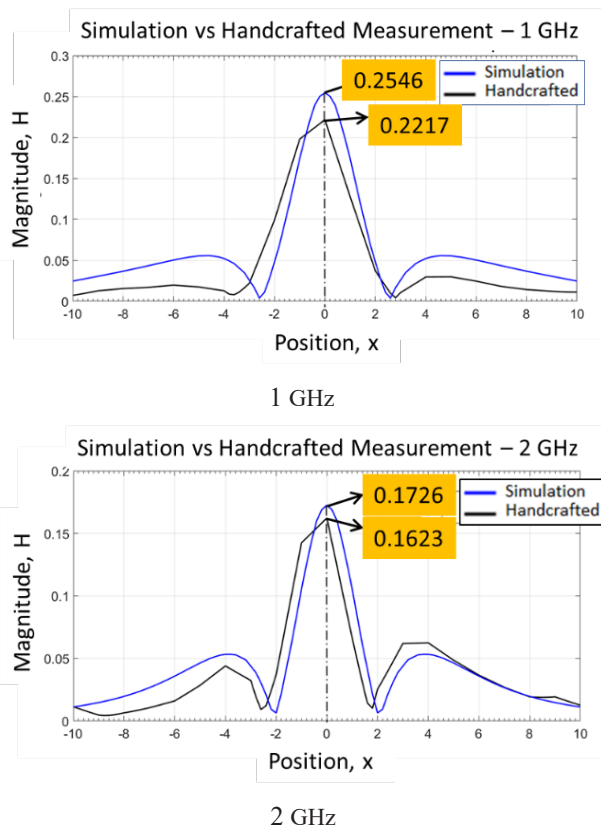


FIGURE 19. Simulation and handcrafted probes in the H-signal ( $S_{21}$ ) for the frequencies 1 GHz and 2 GHz

However, it is still unable to function well after the frequency 2.644 GHz. Even though, the probe factor was applied into the measured voltage and then converted into field strength, the waveform was still abnormal to be compared to simulated one. Figure 20 shows the simulated and measured values of  $S_{21}$  at a frequency of 3 GHz after applying the PF to the measured voltage. This might be due to the asymmetrical handcrafted loop, which affects the sensitivity and frequency response of the result in measurement.

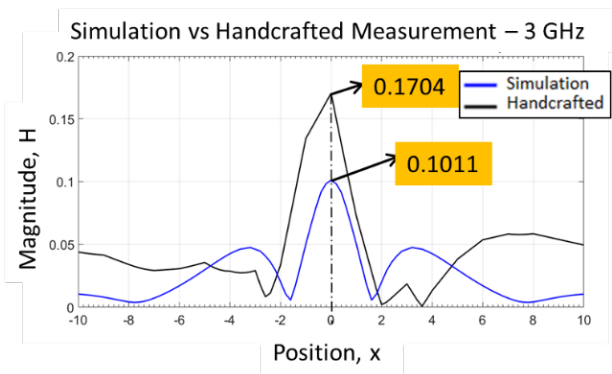


FIGURE 20 Simulation and handcrafted probes in the H-signal ( $S_{21}$ ) for the frequency of 3 GHz

Overall, the ability of the handcrafted probe to detect the radiated field is satisfactory, but must be improved in terms of data sample, surrounding field distribution and the use of the microstrip board. The handcrafted loop probe is still able to identify and detect the near-field radiated from the plane of the microstrip line before it reaches the frequency of 2.644 GHz.

### CONCLUSION

In this research, a functional magnetic field probe was successfully developed for the near-field scanning. Meanwhile, a commercial probe was also used as a comparator in order to assess the ability of both probes to detect near-field disturbances. The magnetic field component corresponds to the output of the measurement probes. Furthermore, a 3D model of the microstrip line was constructed for generating the simulation results. The calibration measurements described in the frequency domain were carried out successfully. Under suitable conditions, it has been shown that the low-cost handcrafted magnetic field probe can perform as well as the more expensive commercial probes. Future works should include designing the magnetic field probe as a printed circuit magnetic probe to further improve its performance. The validation measurement was successfully carried out with the accurate PF based on the measurement and simulation results. Through this study, more studies applying the algorithm development with MATLAB process were initiated to help solve certain equation application problems. Last but not least, so as to obtain more accurate results, the calibration measurement must be conducted under a less reflective radiation environment.



## ACKNOWLEDGEMENTS

The authors would like to acknowledge the support provided by Geran Universiti Penyelidikan UKM (GUP-2019-021) and Geran Galakan Penyelidik Muda UKM (GGPM-2020-005).

## DECLARATION OF COMPETING INTEREST

None

## REFERENCES

- Ag, A. 2020. RF Field-Probes measure E & H fields. [http://www.dtechsolutions.com/product\\_details.php?category\\_id=89&item\\_id=60](http://www.dtechsolutions.com/product_details.php?category_id=89&item_id=60)
- Brochure. 2020. Microwave Modes of a Microstrip Line. [https://www.photond.com/products/fimmwave/fimmwave\\_applications\\_09.htm](https://www.photond.com/products/fimmwave/fimmwave_applications_09.htm)
- Dimitrijević, T., Dimitrijević, T., Atanaskovic, A., Dončov, N. S., Thomas, D. W. P., Smartt, C. & Baharuddin, M. H. 2019. Calibration of the loop probe for the near-field measurement. *International Journal of Microwave and Wireless Technologies (May)*: 567–570. doi:10.1017/S1759078720000690
- Electrotechnical, I. & Commission. 2014. PD IEC/TS 61967-3:2014 Integrated circuits — Measurement of electromagnetic emissions Part 3: Measurement of radiated emissions — Surface scan method.
- Hacker, J. & Gmbh, L. E. 2020. Surface Scan on IC level with high resolution 1–11. <https://www.signalintegrityjournal.com/articles/1752-surface-scan-on-ic-level-with-high-resolution>
- Huang, W. 2019. S-Param: Various indicators ILFit, ILD. <http://www.spisim.com/blog/s-param-various-indicators-ilfit-ild-icn-icr-imr-inext-pqm-rqm/>
- Li, L., Pan, J., Hwang, C., Cho, G., Park, H., Zhang, Y. & Fan, J. 2015. Near-field coupling estimation by source reconstruction and Huygens's equivalence principle. *2015 IEEE Symposium on Electromagnetic Compatibility and Signal Integrity, EMCSI 2015* 324–329. doi:10.1109/EMCSI.2015.7107708
- Neilhao. 2013. Measuring EMI with Homemade Magnetic Field Probe. [Http://Uniteng.Com/Index.Php/2013/05/30/Measuring-Emi-With-Homemade-Magnetic-Field-Probe/](http://Uniteng.Com/Index.Php/2013/05/30/Measuring-Emi-With-Homemade-Magnetic-Field-Probe/). <http://uniteng.com/index.php/2013/05/30/measuring-emi-with-homemade-magnetic-field-probe/>
- Oliveira, F. 2018. DIY Near Field Probes & Preamplifiers 1–12. <https://interferencetechnology.com/diy-near-field-probes-preamplifiers/>
- Purcell, E. M. & Morin, D. J. 2013. Electricity and Magnetism. 3<sup>rd</sup> edition. Cambridge: Cambridge University Press. doi: 10.1017/CBO9781139012973
- Roy Ediss, Philips Semiconductors, U. 1939. Probing the Magnetic Field Probe. “*The Screen Loop Aerial*”, *Wireless Eng. Vol.16*, p. 492, October 1939 Vol. 16. Retrieved from [http://www.compliance-club.com/archive/old\\_archive/030718.htm](http://www.compliance-club.com/archive/old_archive/030718.htm)
- Shrestha, A. 2009. Visible-Light Communication Demonstrator: System modeling and analogue distribution network 1–84. Retrieved from <https://pdfs.semanticscholar.org/8833/019cf029f83120f8da b22fa1717dd3984899.pdf>
- Siegel, D. M. & Siegel, D. M. 2009. Drafts of “A Dynamical Theory of the Electromagnetic Field.” *Innovation in Maxwell's Electromagnetic Theory* (January): 180–181. doi:10.1017/cbo9780511529290.011
- Sivaraman, N. 2017. Design of magnetic probes for near field measurements To cite this version: HAL Id : tel-01757038 Design of magnetic probes for near-field measurements and the development of algorithms for the prediction of EMC.
- Team, T. A. 2017. Stripline vs Microstrip: Understanding Their Differences and Their PCB Routing Guidelines 2–5. <https://medium.com/@Altium/stripline-vs-microstrip-understanding-their-differences-and-their-pcb-routing-guidelines-9bad77303d2f>
- Zhang, J., Kam, K. W., Min, J., Khilkevich, V. V., Pommerenke, D. & Fan, J. 2013. An effective method of probe calibration in phase-resolved near-field scanning for EMI application. *IEEE Transactions on Instrumentation and Measurement* 62(3): 648–658. doi:10.1109/TIM.2012.2218678